SI Materials and Methods

Cell culture Cell lines were maintained in high glucose DMEM medium (Sigma-Aldrich) supplemented with 20 % (v/v) fetal bovine serum (FBS) (Sigma-Aldrich), 100 U/ml penicillin, 100 U/ml streptomycin (Life technology), 2 mM glutamine (Life technology), 1 % (v/v) Non-essential amino acid (Life technology), and 0.1 % (v/v) 2-mercaptoethanol (Life technology) and reached the log phase of growth prior to performing the triggering experiment. Naïve T cells from mice were isolated and used shortly post-purification as described below.

Production and characterization of N15 αβ and NP63 αβ T cell lines and their IL-2 production The BW5147.3 cell line was obtained from ATCC and plasmids CD3δγεζWT pMIY and TCR αβ pMIG were a kind gift from the D. Vignali (St. Jude Children's Research Hospital, Memphis, Tennessee). The wildtype mouse CD3 and N15 TCR genes in each plasmid were constructed using the viral 2A-linked system (1) to generate multicistronic vectors for co-transfection of all of the CD3 and TCR genes. The CD8α and β genes (2) was sub-cloned into the pcDNA3.1 vector and then transfected into the BW5147.3 cell line to generate BW5147.3-CD8 αβ. To next generate the N15 αβ TCR expressing cell line, the CD3δγεζ WT and N15 TCR αβ plasmids were first transfected into Pheonix-Eco packing cells for the production of CD3 and TCR retroviruses. The virus supernatants were harvested and then used to retrovirally transduce the BW5147-CD8 αβ cells to incorporate the CD3 and TCR genes in that order to create the N15TCRαβ + CD8α +CD8β +BW5147.3 cell line (N15 αβT cells). For a second αβ T cell line, NP63, a similar approach was employed. The NP63 TCR is an influenza A PR8 virus $NP_{366\text{-}374}$/H-$2D^b$-specific αβTCR cloned from PR8 virus infected mice, as shall be detailed in a subsequent paper. Briefly, however, $CD8^+$ $NP_{366\text{-}374}$/H-$2D^b$ $tetramer^+$ cells from spleen of influenza infected mice were single-cell sorted and TCRα and β cDNAs were amplified from individually sorted cells by single-cell RT-PCR method (3, 4). Both N15 and NP63 T

cell lines were sorted by FACS for stable TCR expression at copies representative of normal naïve or memory αβ T cells (~20,000-40,000 copies per cell).

The T cell activation assay was carried-out in triplicate in a 96 well plate using 1-2×10^5 R8 cells irradiated at 3000 rads prior to use with 1-2×10^5 N15 or NP63 T cells in each well. Varying concentrations of the stimulatory peptides VSV8, L4 or NP366 were added to each well ranging from 0-10 μg/ml. An optimal combination of PMA (25 ng/ml)/ionomycin (2.5 μg/ml) was used as a positive control. The peptide stimulated cells and the negative and positive controls were incubated for 16-18 hours overnight at 37 °C. Following incubation, the cell supernatants were harvested for IL-2 ELISA assay. Where indicated, the EC50 of the IL-2 producing cells was calculated using a 4-parameter logistic model (5).

The IL-2 ELISA assay was completed using the mouse IL-2 DuoSet and ancillary reagent kit 2 (R&D systems). The T cell supernatants were diluted in media such that the O.D. 450 nm readings fall within the standard curve for the assay due to the high level of IL-2 production in the presence of the VSV8 peptide. The assay was then carried out following the kit instructions. The negative control values were subtracted from each sample point and concentrations in pg/ml were calculated from the standard curve.

Preparation of naïve N15Tg CD8⁺ T cells Four 9-16 week old homozygous N15 TCR transgenic (tg) mice on the B6*Rag2*$^{-/-}$ background were used for the isolation of naïve T cells (6). Mice were maintained and bred under specific pathogen-free conditions in the animal facility of the Dana-Farber Cancer Institute under a protocol reviewed and approved by the Animal Care and Use Committee. The naïve CD8⁺ N15 T cells were purified by magnetic sorting using naïve CD8α⁺ isolation kit (Miltenyl Biotec) containing mAbs against CD4, CD11b, CD11c, CD19, CD45, CD49b, CD105, Ter-119, MHCII, CD44 and TCR γδ from spleen of N15 TCRtg Rag2$^{-/-}$ mice

according to the manufacturer's instructions. Post-purification by negative selection, the naïve $CD8^+$ N15 T cells were used without prior stimulation.

Antibodies (Abs) and flow cytometric analysis The following monoclonal antibodies (mAbs) were used: FITC-conjugated anti-Vβ 5.2 (ebioscience), APC-conjugated anti-Vβ 5.2 (MR9.4) (ebioscience), FITC-conjugated anti-TCR Cβ (H57-597) (Biolegend), APC-conjugated anti-TCR Cβ (H57-597) (Biolegend), APC-conjugated anti-CD3ε (145-2C11) (ebioscience), APC-conjugated anti-CD3εγ (17A2) (ebioscience), APC-conjugated anti-CD8α (53-6.7) (Biolegend), APC-conjugated anti-CD8β (53-5.8) (Biolegend) and PE-conjugated anti-H-$2K^b$ antibody (AF6-88.5) (ebioscience). For flow cytometry, single-cell suspensions of the T cells were prepared at 3×10^6 cells/ml in PBS containing 2% FBS. Those cells were single-color stained with the mAbs at saturating concentrations. After incubation on ice for 20 minutes, the stained cells were washed, transferred to falcon tubes and analyzed by flow cytometry immediately using a 3-laser BD LSRII. Dead cells were excluded by forward and side scatter gating. For determining TCR expression, FITC-conjugated anti-Vβ and/or H57 mAb were utilized. Mean fluorescence intensities (MFI) were calculated based on the fluorescence method by FACS and the average number of TCRs per cell is ~$2\text{-}4\times10^4$ (7).

pMHC coated beads The vesicular stomatitis virus nuclear protein octapeptide (VSV8, RGYVYQGL) which is the cognate antigen (in complex with H-$2K^b$) for the N15 TCR was bound to recombinant H-$2K^b$ containing a C-terminal biotinylation tag (GGGLNDIFEAQKIEWH) (8). In addition to the strong agonist peptide VSV8, the weak agonist L4, which contains a single valine-to-leucine substitution at the p4 position of VSV8, or the unrelated Sendai virus nonamer peptide SEV9 was also used to complex with the recombinant H-$2K^b$. SEV9 binds to K^b with comparable affinity to VSV8 but is unable to activate N15TCR-expressing T cells (9, 10). The streptavidin (SA)-coupled polystyrene beads (1.09 μm diameter, Spherotech) were washed with PBST buffer (1X PBS without calcium (cellgro) with 0.02% (v/v) Tween-20 (Sigma-

Aldrich)) three times. To create sample beads with distinct pMHC densities, different concentrations of biotinylated VSV8/K^b solutions were added to the SA-coupled polystyrene bead solution and gently rotated for 1h at room temperature and then wash three times by PBST. For 2×10^5 VSV8/K^b molecules/bead sample, 5 μl of 10 μM of H-2K^b complexes were used for coupling to 5 μl 0.01% w/v streptavidin polystyrene beads. For 2×10^4, 200, 20 and 5 VSV8/K^b molecules/bead samples, 1 μM, 100 nM, 10 nM and 2.5 nM concentrations of H-2K^b complexes were used for coupling to 5 μl 0.1% w/v streptavidin polystyrene beads. For T cell triggering, bead surfaces were blocked by adding 5 mg/ml 20 μl biotin-BSA (ThermoFisher) in the pMHC coated bead slurry for 1h at room temperature and then wash three times by PBST. The BSA on the bead surface eliminates potential non-specific binding of the bead to the cell membrane (11). For the assays with two beads, the SA-coupled polystyrene beads (1.25 μm diameter, spherotech) were used following the same coating procedure as above. The biotinylated wild type VSV8/H-2K^b, L4/H-2K^b and SEV9/H2-K^b and the biotinylated mutant VSV8/H-2$K^b{}_m$ and NP366/H-2$D^b{}_m$ molecules whose CD8 coreceptor binding sites were eliminated (both mutants obtained from the NIH Tetramer Core Facility) were used in identical bead-coating procedures.

Quantitation of pMHC on the bead surface Quantitative immunofluorescence was used to determine the densities of pMHC on the bead surface (7). When the number of VSV8/K^b on the bead surface is above 500, different amounts of PE-conjugated anti-H-2K^b antibody (AF6-88.5) was added into the bead solution. After 1-hour gentle rotation, the stained beads were examined by flow cytometry with Mode values of mean fluorescence recorded and normalized by dividing the maximum fluorescence signal using 0.1 μg antibody. It is estimated that the interacting surface between the bead and the cell represents up to ~10% of the bead surface area and 10% was used when the surface expression is at 2×10^5 pMHC/bead (12).

Flow cytometry reached its limitation of distinguishing the pMHC bead signal from the background if the surface expression is equal to or lower than 500 pMHC/bead. Accordingly, at low density we used the single molecule total internal reflection fluorescence (smTIRF) microscopy method with a penetration depth of ~400 nm easily able to sample the relevant interface contacting the cell surface. Saturated amount of PE-conjugated anti-H-2K^b antibody (AF6-88.5) was added into the bead solution, gently rotated for 1-hour. The stained beads were washed with PBST three times, resuspended in 1X PBS buffer and then examined by smTIRF microscopy.

The methodology for calculating the pMHC copies at the interface is as follows with 200 pMHC coated bead used as a representative example. A flow cell containing two separate channels was created where one channel was loaded with 200 pMHC copy-coated beads labeled with PE-conjugated anti-H-2K^b antibody (AF6-88.5) and the other channel loaded with streptavidin beads labeled with the same antibody to calibrate the non-specific binding between antibody and SA. After loading the beads, each channel was washed with 1X PBS five times. Fluorescence signals of single PE-conjugated anti-H-2K^b antibody and background were obtained from bead images.
The following three equations are used in calculations where *I* represents the mean fluorescence intensity:

$$I_{\text{200pMHC/bead}} = n \times I_{\text{single PE-mAb}} + I_{\text{nonspecific binding between SA bead and mAb}} + I_{\text{Background}} \quad (1)$$

$$I_{\text{nonspecific binding}} = I_{\text{nonspecific binding between SA bead and mAb}} + I_{\text{Background}} \quad (2)$$

$$I_{\text{PE-mAb}} = I_{\text{single PE-mAb}} + I_{\text{Background}} \quad (3)$$

The same region of interest was selected to include pMHC coated bead ($I_{\text{200pMHC/bead}}$), SA-bead ($I_{\text{nonspecific binding}}$), PE-conjugated anti-H-2K^b antibody ($I_{\text{PE-mAb}}$), or the background ($I_{\text{Background}}$) and the mean fluorescence intensities were determined, i.e. the left parameters in all three equations. *n* is the number of pMHC molecules at the interface.

Expressions of $I_{\text{nonspecific binding between SA bead and mAb}}$ and $I_{\text{single PE-mAb}}$ in eq 1 can be obtained from eq 2 and 3 and then by introduction of the $I_{\text{Background}}$ value, one derives

$$n = \frac{I_{\text{200 pMHC bead}} - I_{\text{SA bead}}}{I_{\text{PE-mAb}} - I_{\text{Background}}} \tag{4}$$

From eq 4, the average numbers of VSV8/K^b at the interface are 29, 2 and 0.5 VSV8/K^b based on different seeding amounts of VSV8/K^b despite coating number estimates of 200, 20 and 5, respectively.

Half-antibody coated beads The half-anti-TCRVβ 5.2 (MR9.4) mAb was produced as previous described (13). After desalting and changing the buffer to 1X PBS (cellgro, pH=7.4), ~0.1 mg of the digestion product was incubated with Biotin-maleimide (Sigma-Aldrich) in 20-fold molar excess. The solution was retained and rotated at 4 °C overnight. The reaction was terminated by desalting and a biotin tag was added to the hinge region of the half-antibody. The half-antibody solution was further diluted to the desired concentration to make the half-antibody coated beads. Identical procedures described above for preparation of VSV8/K^b coated beads were used to prepare beads coated with 5 half-antibody molecules to get a 0.5 molecules per cell-bead interface number.

Antibody-coated fluorescence beads 5 μl *SA*-coupled polystyrene beads (0.1% w/v, 1.03 μm diameter, spherotech) were washed by PBST buffer three times. 10 nM biotin-conjugated anti-CD3εγ (17A2) (Biolegend) were added in the bead slurry and gently rotated for 1h at room temperature and then washed three times by PBST. 2 μl 10 mg/ml dextran with tetramethylrhodamine (TT) and biotin (MW=3 kDa, ThermoFisher) was added to the antibody coated bead slurry and gently rotated for 1h at room temperature and then washed three times by PBST. The negatively charged dextran inhibits nonspecific binding between the cell membrane and the bead.

Ca^{2+} flux dye loading Because TCR signaling is associated with elevations in intracellular free calcium, the Quest Rhod-4, AM (AAT Bioquest, Inc.) was used to stain the T cell and observe the characteristic intracellular calcium flux during T cell triggering (14). Briefly, cells were washed, resuspended at 2 million cells/ml in either colorless DMEM medium (Sigma-Aldrich) for cell lines or colorless RPMI 1640 (Life technology) for naïve cells, and loaded with Quest Rhod-4 at 2 μM for 40 min in the presence of 3% (v/v) FBS, 0.02% (v/v) Pluronic F-127 (Sigma-Aldrich) in PBS at 37 °C. Cells were gently pipetted every 10 min. T cells were then washed by 1 ml colorless DMEM medium, resuspended in 800 μl colorless DMEM (cell line) or colorless RPMI 1640 (naïve cell) with 3% (v/v) FBS and transferred to a cover glass flow cell for 1 h incubation at 37 °C, 5% CO_2 to allow for cell attachment to the cover glass surface. After coating the surface with blocking buffer containing 5 mg/ml BSA (Sigma-Aldrich) in colorless DMEM medium for 10 min, pMHC-coated beads in blocking buffer were flowed into the sample. After 1h incubation at 37 °C, 5% CO_2, the slide was ready for manipulation using an optical trap combined with fluorescence.

Estimation of Ca^{2+} concentration change during TCR triggering under load Estimating the Ca^{2+} concentration change during TCR triggering was difficult due to nonlinearities and saturation of fluorescence signal of the Andor camera. Traditionally the method involves the following calculation:

$[Ca^{2+}] = K_d * (F - F_{min})/(F_{max}-F)$

where F is the fluorescence of the indicator at experimental calcium levels, F_{min} is the fluorescence in the absence of calcium and F_{max} is the fluorescence of the calcium-saturated probe. Quest Rhod-4 has a K_d equal to 525 nM. In our case, the precise value of the positive control to obtain F_{max} cannot be determined due to saturation of the fluorescence signal of the Andor camera.

However, we obtained F_{min} from the Andor camera with identical excitation laser power (532 nm) and camera gain to our measurements. Using an identical

procedure for sample preparation and Ca^{2+} dye loading as in our experiments, we changed our imaging buffer to a 1X PBS containing 3% FBS and 2mM EDTA (sigma). This permitted measurement of the average fluorescence levels in cells loaded with the Ca^{2+} chelating agent resulting in an intensity ~0.8 times the basal signal (n=50 cells). Given the original concentration of Ca^{2+} is ~50 nM (15), F_{max} is calculated to be ~3.1 times higher than the basal fluorescence. Since signal changes for T cells in our measurements were ~1.2 times on average (**Figs. 2A and B**) we estimate a concentration of ~111 nM Ca^{2+} is present in stimulated T cells under optimal load using pMHC coated beads.

Antibody and drug treatment of T cells For the H57 Fab treated experiment, 0.5 μl 1 mg/ml H57 Fab was added into the cell slurry after the 40-min dye-loading procedure and kept at 37 °C, 5% CO_2 for 20-min before loading slurry into flow cell. H57 Fab was always present at a concentration of 4.5 μg/ml (i.e. 1000-fold excess of TCR number).

For drug treatment experiments, reagent was firstly dissolved in DMSO (Sigma-Aldrich) and then dilute to its final concentration in the blocking buffer containing 5 mg/ml BSA. The final concentrations of drugs are 500 nM Cytochalasin D (Santa Cruz Biotechnology), 10 μM Nocodazole (Sigma-Aldrich) and 25 μM (S)-(-)-Blebbistatin (Santa Cruz Biotechnology). After 1h incubation at 37 °C, 5% CO_2, the slide was ready for manipulation using a trapping beam (1064 nm). Drugs were always present in the slides at their final concentrations during the triggering experiment. The DMSO amount in the final solution is lower than 0.2% (v/v) to maintain the cell viability and functionality.

Cell loaded slide preparation Slides were prepared by first creating a 110 μl flow cell using two layers of double-sided sticky tape. The flow cell is then loaded through capillary action with the final calcium dye loaded cell solution. In all cases the cell is nonspecifically immobilized on the coverslip surface by maintaining the

loaded chamber at 37 °C, 5% CO_2 (~1 h). We note that these measurements are in the low Reynolds number regime where viscous forces dominate over inertial forces. Relative motions are slow with maximum speeds of the piezo stage 2 μm/s. Given these speeds, viscosity of the medium (DMEM medium is 0.78×10^{-3} N•s/m^2), density of the fluid (1.0×10^3 kg/m^3) and length scale of the channel (179 μm tall channel and 1 μm diameter bead) we conservatively estimate the Reynolds number is < 5×10^{-4} and drag on the bead below 0.015 pN. Control measurements using beads with no pMHC but coated with BSA executed the similar relative motions of bead and cell apposition and showed no triggering.

Two-bead assay. A single 17A2 antibody functionalized fluorescently labeled bead (d=1.03 μm) was firstly trapped with a 1,064-nm laser and then placed alongside a surface-bound T cell with an automated piezoelectric stage. Secondly, a saturated VSV8/K^b -coated bead (d=1.25 μm) was trapped and placed at a position 2 μm distal to the antibody-coated bead. This distance ensures that the trap does not interfere with the antibody-coated bead. Immediately following attachment of the the saturated VSV8/K^b -coated bead to the T cell membrane, the trap laser was turned off and T cells were excited using a 532-nm laser to monitor Ca^{2+} sensitive Quest Rhod-4 fluorescence every 4 sec. Two DIC images were also taken before and after the 10-min fluorescence recoding. Assays were performed at 37 °C.

Calculation of elastic moduli and viscosities from force relaxation experiment
Fig. S7A shows the viscoelastic model used to represent the cell's behavior. In this model the strain can be split into the sum of three terms:

$$\varepsilon_T = \varepsilon_0 + \varepsilon_{D1} + \varepsilon_{S1} \tag{1}$$

Also we have the following equations for all the stresses in this model:

$$\sigma = \sigma_0 = \sigma_1 + \sigma_2 \tag{2}$$

$$\sigma_0 = \eta_0 \dot{\varepsilon}_0 \tag{3}$$

$$\sigma_1 = \eta_1 \dot{\varepsilon}_{D1} = E_1 \varepsilon_{S1} \tag{4}$$

$$\sigma_2 = E_2(\varepsilon_{D1} + \varepsilon_{S1}) \tag{5}$$

Substituting eq 5 into eq 1 and then differentiating once this equation we can get the following equation:

$$\dot{\varepsilon}_T = \frac{\sigma}{\eta_0} + \frac{\dot{\sigma} - \dot{\sigma}_1}{E_2} \tag{6}$$

Differentiating once eq 4 and after substituting it into eq 6 we can obtain the following two equations:

$$\dot{\varepsilon}_T = \frac{\sigma}{\eta_0} + \frac{\dot{\sigma} - \eta_1 \ddot{\varepsilon}_{D1}}{E_2} \tag{7}$$

$$\dot{\varepsilon}_T = \frac{\sigma}{\eta_0} + \frac{\dot{\sigma} - E_1 \dot{\varepsilon}_{S1}}{E_2} \tag{8}$$

For the stresses, we can substitute eqs 4 and 5 into eq 2 and then differentiate once this equation. The equation would be:

$$\dot{\sigma} = E_1 \dot{\varepsilon}_{S1} + E_2 \left(\dot{\varepsilon}_{S1} + \dot{\varepsilon}_{D1} \right) \tag{9}$$

Then the expression of $\dot{\varepsilon}_{S1}$ would be obtained in the form as:

$$\dot{\varepsilon}_{S1} = \frac{\dot{\sigma} - E_2 \dot{\varepsilon}_{D1}}{E_1 + E_2} \tag{10}$$

Plugging eq 10 into eq 8 we can get the following equation:

$$\dot{\varepsilon}_T = \frac{\sigma}{\eta_0} + \frac{\dot{\sigma} + E_1 \dot{\varepsilon}_{D1}}{E_1 + E_2} \tag{11}$$

We can get $\dot{\varepsilon}_{D1}$ and then we take its second derivative form into consideration:

$$\ddot{\varepsilon}_{D1} = \frac{E_1 + E_2}{E_1} \left(\ddot{\varepsilon}_T - \frac{\sigma}{\eta_0} \right) - \frac{\ddot{\sigma}}{E_1} \tag{12}$$

On the optical trap side, we can get the total stress as:

$$\sigma = k_{trap}\left(\mathrm{x}_0 - \varepsilon_T\right) \tag{13}$$

where k_{trap} is the stiffness of trap and x_0 is the initial distance between bead and trap center.

We consider its first and second derivative form:

$$\dot{\sigma} = -k_{trap}\dot{\varepsilon}_T \tag{14}$$

$$\ddot{\sigma} = -k_{trap}\ddot{\varepsilon}_T \tag{15}$$

Substituting eqs 12, 13, 14 and 15 into eq 7 we can obtain a linear homogeneous ordinary differential equation with constant coefficients

$$\left[\frac{\eta_1\left(E_1+E_2\right)}{E_1E_2k_{trap}} + \frac{\eta_1}{E_1+E_2}\right]\ddot{\sigma} + \left[\frac{\eta_1\left(E_1+E_2\right)}{\eta_0E_1E_2} + \frac{1}{k_{trap}} + \frac{1}{E_2}\right]\dot{\sigma} + \frac{\sigma}{\eta_0} = 0 \tag{16}$$

The general solution to the homogeneous equation $A\ddot{\sigma} + B\dot{\sigma} + C\sigma = 0$ is given by $\sigma(t) = C_1e^{-t/\tau_1} + C_2e^{-t/\tau_2}$. We also have two time boundary conditions at t=0 and t=t_f. The latter is the time when bead snapping back to the trap center.

During the fitting process, the fitting equation should be restricted by the two conditions $C_1 + C_2 = \sigma(0)$ and $C_1e^{-t/t_f} + C_2e^{-t/t_f} = 0$. We also found out one part of this expression can be neglected as absolute value of either C_1 or C_2 is extremely close to zero and its associated decay constant is at least 10000 times greater than the other one. Therefore, the fitting equation can be simplified to:

$$\sigma(t) = Ce^{-t/\tau} \tag{17}$$

When normal force is applied to the system, the model would be changed to Zerner's model and usually the bead never goes back to the trap center as shown in **Fig. S9B**. The general solution to this model was well described in Moreno-Flores's paper (16). Basically, it has the expression as $\sigma(t) = C_0 + C_1e^{-t/\tau_1} + C_2e^{-t/\tau_2}$. Detailed discussion on all the parameters is beyond the content of this paper but can be provided by requesting information from the authors.

Data Analysis The step finding script was modified from a previous version within the lab and based on a sliding Student's t-test that detects the edges of each step to prescribe a dwell and allows for varied step sizes (17). A dwell was defined as a period of constant position between bursts of motion (steps). Specifically, a dwell is identified if the change in the moving average of position is less than 5 nm (the minimum step-size threshold). This threshold was chosen as a result of step finding optimization. Dwell locations were determined through averaging all points within the dwell period. After dwell optimization, starting and ending times of each dwell were recorded and plotted with the dwell location. It is also noted that step analysis for each trace was visually inspected for accuracy. The same analysis conditions were used for all traces in a data set. In some cases, steps were not always identified as commonly observed for Blebbistatin treated cells. Less frequently, other treatments revealed step loss due to the low signal to noise level. However, these traces are still used to calculate the average number of steps per trace. To avoid the differences of pulling distance for each condition (H57 Fab, drugs or NP366/D^b), the total pulling distances for every condition were normalized to the distances of N15 T cell with 2 VSV8/K^b at interface.

In order to confirm the existence of the discrete steps ~8 nm in wt T cells and the reduction in Blebbistatin (Blebb) treated cells, point to point pairwise distance differences were calculated followed by spatial frequency analysis. Five representative traces were selected and individually fit to an exponential decay to remove extension due to compliance in the trace. The residual of each trace was calculated to remove the decay and the pairwise distance differences function of the subtract trace was calculated. The power spectrum derived from each pairwise function(18, 19), was normalized and pooled to create an average power spectrum.

References

1. Szymczak AL, *et al.* (2004) Correction of multi-gene deficiency in vivo using a single 'self-cleaving' 2A peptide-based retroviral vector. *Nat Biotech* 22(5):589-594.
2. Chang H-C, *et al.* (2005) Structural and Mutational Analyses of a CD8αβ Heterodimer and Comparison with the CD8αα Homodimer. *Immunity* 23(6):661-671.
3. Hamana H, Shitaoka K, Kishi H, Ozawa T, & Muraguchi A (2016) A novel, rapid and efficient method of cloning functional antigen-specific T-cell receptors from single human and mouse T-cells. *Biochemical and Biophysical Research Communications* 474(4):709-714.
4. Kobayashi E, *et al.* (2013) A new cloning and expression system yields and validates TCRs from blood lymphocytes of patients with cancer within 10 days. *Nat Med* 19(11):1542-1546.
5. Sebaugh JL (2011) Guidelines for accurate EC50/IC50 estimation. *Pharmaceutical Statistics* 10(2):128-134.
6. Ghendler Y, *et al.* (1997) Double-positive T cell receptorhigh thymocytes are resistant to peptide/major histocompatibility complex ligand-induced negative selection. *European journal of immunology* 27(9):2279-2289.
7. Carpentier B, Pierobon P, Hivroz C, & Henry N (2009) T-Cell Artificial Focal Triggering Tools: Linking Surface Interactions with Cell Response. *PLoS One* 4(3):e4784.
8. Moody AM, Xiong Y, Chang H-C, & Reinherz EL (2001) The CD8αβ co-receptor on double-positive thymocytes binds with differing affinities to the products of distinct class I MHC loci. *European journal of immunology* 31(9):2791-2799.
9. Sasada T, *et al.* (2003) Disparate peptide-dependent thymic selection outcomes in β2M-deficient mice versus TAP-1-deficient mice: implications for repertoire formation. *European journal of immunology* 33(2):368-380.
10. Sasada T, Ghendler Y, Wang and J-h, & Reinherz EL (2000) Thymic selection is influenced by subtle structural variation involving the p4 residue of an MHC class I-bound peptide. *European journal of immunology* 30(5):1281-1289.
11. Alon R, Bayer EA, & Wilchek M (1993) Cell adhesion to streptavidin via RGD-dependent integrins. (Translated from eng) *Eur J Cell Biol* 60(1):1-11 (in eng).
12. Amin L, Ercolini E, Shahapure R, Bisson G, & Torre V (2011) The elementary events underlying force generation in neuronal lamellipodia. *Scientific reports* 1:153.
13. Das DK, *et al.* (2015) Force-dependent transition in the T-cell receptor β-subunit allosterically regulates peptide discrimination and pMHC bond lifetime. *Proceedings of the National Academy of Sciences* 112(5):1517-1522.
14. Freedman MH (1979) Early biochemical events in lymphocyte activation. *Cellular Immunology* 44(2):290-313.

15. Jensen WA*, et al.* (1997) Qualitatively distinct signaling through T cell antigen receptor subunits. *European journal of immunology* 27(3):707-716.
16. Susana M-F, Rafael B, María d MV, & José Luis T-H (2010) Stress relaxation and creep on living cells with the atomic force microscope: a means to calculate elastic moduli and viscosities of cell components. *Nanotechnology* 21(44):445101.
17. Brady SK, Sreelatha S, Feng Y, Chundawat SPS, & Lang MJ (2015) Cellobiohydrolase 1 from Trichoderma reesei degrades cellulose in single cellobiose steps. *Nature Communications* 6:10149.
18. Aubin-Tam M-E, Olivares AO, Sauer RT, Baker TA, & Lang MJ (2011) Single-molecule protein unfolding and translocation by an ATP-fueled proteolytic machine. *Cell* 145(2):257-267.
19. Svoboda K, Schmidt CF, Schnapp BJ, & Block SM (1993) Direct observation of kinesin stepping by optical trapping interferometry. *Nature* 365(6448):721-727.

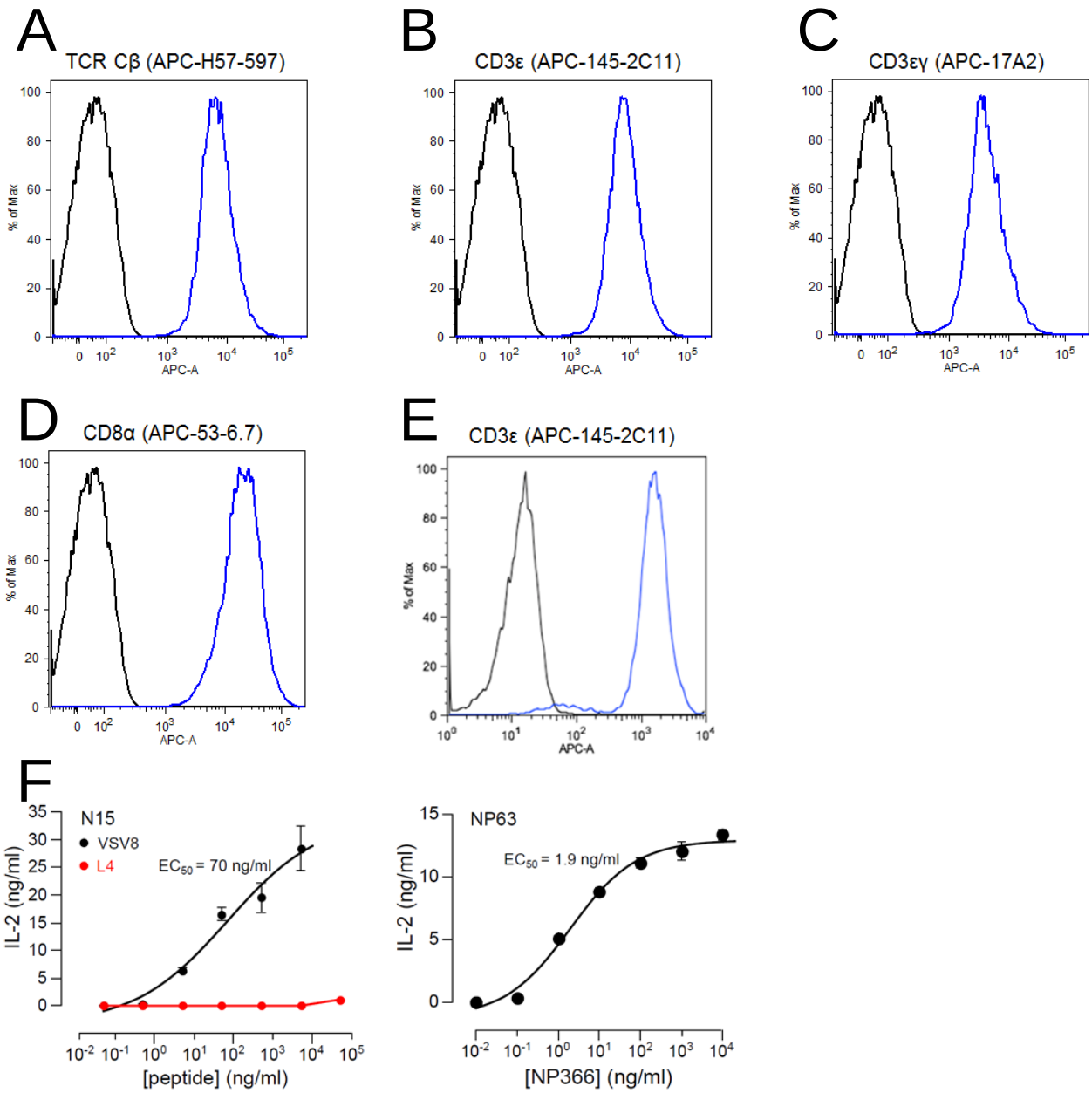

Fig. S1. Supplemental analysis of TCR transfectants. Flow cytometry confirms surface expression of (**A**) TCRβ constant domain and (**B**) CD3*ε*, (**C**) CD3*εγ* and (**D**) CD8*α* on N15 T cells. (**E**) CD3*ε* expression of NP63 T cells. Black curves in histograms A-E show background staining of the cells in the absence of antibody. (**F**) IL-2 production from N15 T cells and NP63 T cells with the indicated peptides as stimulators. Results shown represent mean and standard deviations (SD) of triplicate samples. Note that when the SD is very small, it is not visible in this display. The only L4 concentration stimulating IL-2 production

above background is at 50 μg/ml ($p<0.001$), consistent with prior studies (**Refs. 9-10** in ***SI Materials and Methods***). EC_{50} values are given for VSV8/K^b and NP366/D^b for N15 and NP63 TCRs, respectively.

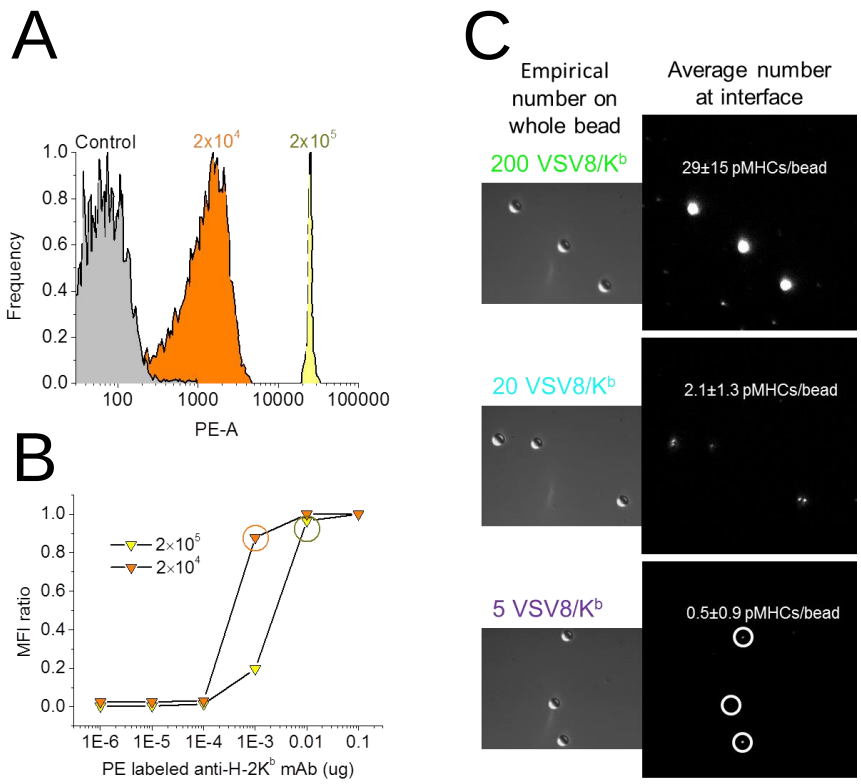

Fig. S2. Flow cytometric and single molecule TIRF fluorescence imaging analysis of indicated H-2K^b complexes with different numbers of pMHC molecules immobilized on beads.

(A) FACS fluorescence signals of 2×10^5 and 2×10^4 coated beads.

(B) Serial dilutions of mAb for measuring the surface copy numbers of 2×10^5 and 2×10^4 VSV8/K^b-coated beads with the inflection points (circled) used to calculate the pMHC numbers as indicated below. MFI: mean fluorescence intensity.

(C) Single molecule TIRF fluorescence imaging analysis of beads calculated to display 200, 20 and 5 VSV8/K^b molecules/bead. More than 200 beads were measured and averaged for each empirically determined surface expression analysis. The values in the fluorescence field of view indicate the empirically determined average number +/- SD on the bead-cell contacting surface. Fluorescence signals of background, single dye and bare streptavidin coated beads were also measured. The coupled H-2K^b complexes were quantitated on beads using directly PE-labeled anti-H-2K^b mAb (AF6-88.5) immunofluorescence (anti-K^b-PE).

Detailed bead preparation methods are found in ***SI Materials and Methods*.**

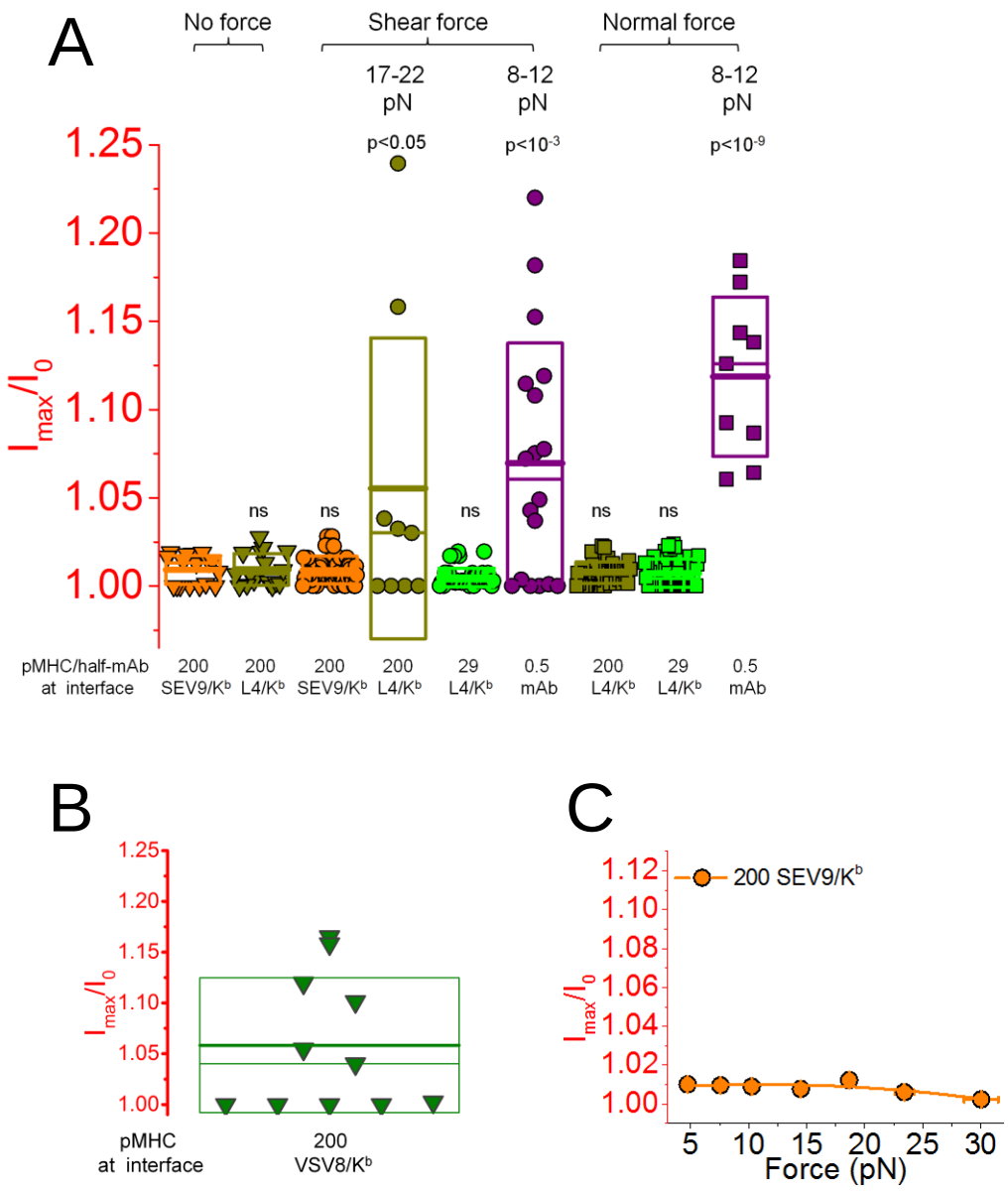

Fig. S3. Thresholds for αβTCR triggering are dependent on ligand species, copy number and directional force.

(A) Ca^{2+} flux was triggered in N15αβ T cells by using either a high L4/K^b copy number at the bead-cell interface (~200) with external shear or 0.5 half anti-TCRVβ antibody (MR9.4) in conjunction with an optimal vectoral force in both normal and shear directions. The other indicated conditions did not trigger. Ca^{2+} flux signal is indicated as the ratio of maximum fluorescence intensity (I_{max}) to the initial fluorescence intensity (I_0) of the Ca^{2+} sensitive dye. The rectangle height illustrates the standard

deviation. Mean value and median value are shown in thick and thin horizontal lines, respectively. *p*-values referring significant analysis were evaluated using One-Way ANOVA for all data points.

(B) N15$\alpha\beta$ T cell triggering of Ca^{2+} flux with 200 VSV8/K^b at the interface.

(C) Directional force vs N15$\alpha\beta$ T cell triggering of Ca^{2+} flux with 200 SEV9/K^b as a function of the load at the interface. Fit curves show lack of a distinct peak. Error bars represent SEM.

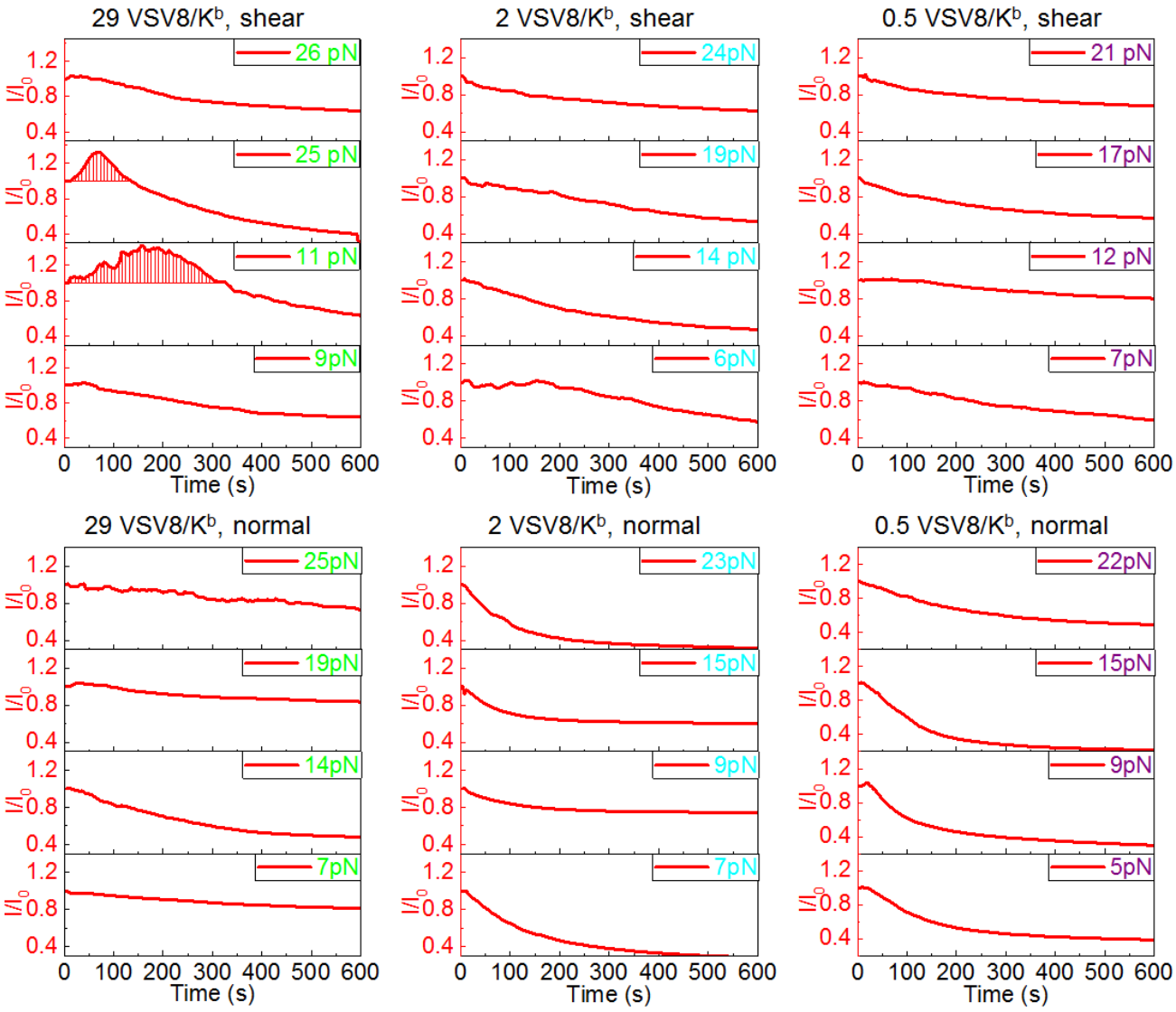

Fig. S4. Representative Ca^{2+} signals at indicated force, vectoral direction and VSV8/K^b copies at the bead-T cell interface. Activation is denoted by the area of red bars under the red Ca^{2+} signal curves.

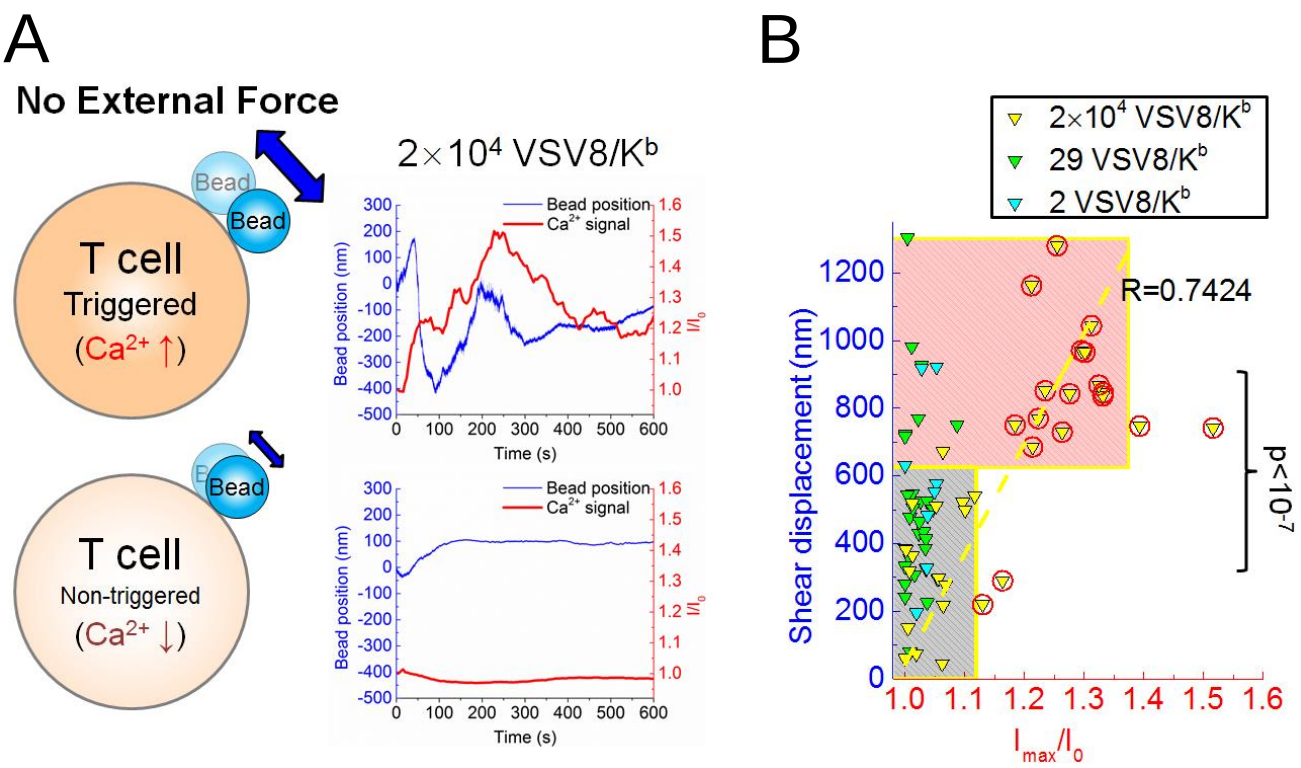

Fig. S5. Relationship between αβTCR triggering and pMHC bead shear displacement in the absence of external force.

(A) Representative 2×10^4 VSV8/K^b bead motion along the shear direction in relationship to contemporaneous measurement of Ca^{2+} signal in a triggered versus a non-triggered T cell, assessed in the absence of external load.

(B) 2×10^4 VSV8/K^b bead displacement along the shear direction correlates with Ca^{2+} signal in N15 T cells triggering in the absence of external load (R=0.7427). In contrast, beads with 29 or 2 copies of VSV8/K^b at the contact interface show no correlation. The red and grey box upper limits represent statistical regions (mean+SD) for triggered vs. non-triggered cells respectively, stimulated with 2×10^4 VSV8/K^b bead. 625 nm shear displacement is used as demarcation. The yellow dash line is the correlation analysis between 2×10^4 VSV8/K^b bead shear displacement and Ca^{2+} signal of TCR triggering. Yellow data points with red circles are T cells defined as "Triggered", whose I_{max}/I_0 is higher than 1.12, which is the upper limit of the grey box. *p*-value refers to the significant difference between values in red and grey boxes evaluated using a One-Way ANOVA.

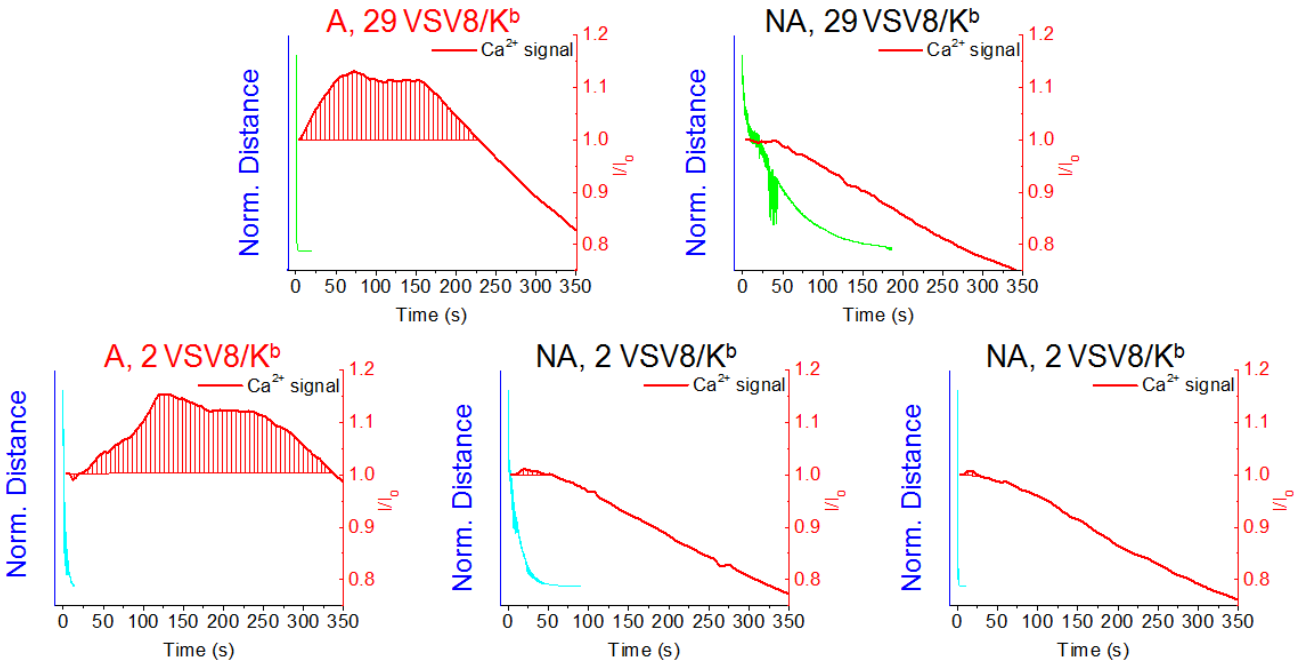

Fig. S6. Optimal external trapping force relaxation along the shear direction depicted with concurrent Ca^{2+} signal of a triggered T cell at 29 VSV8/K^b (top row) and 2 VSV8/K^b (bottom row) conditions. Activated cells are denoted with red bars under the Ca^{2+} signal curves. A, activated. NA, nonactivated.

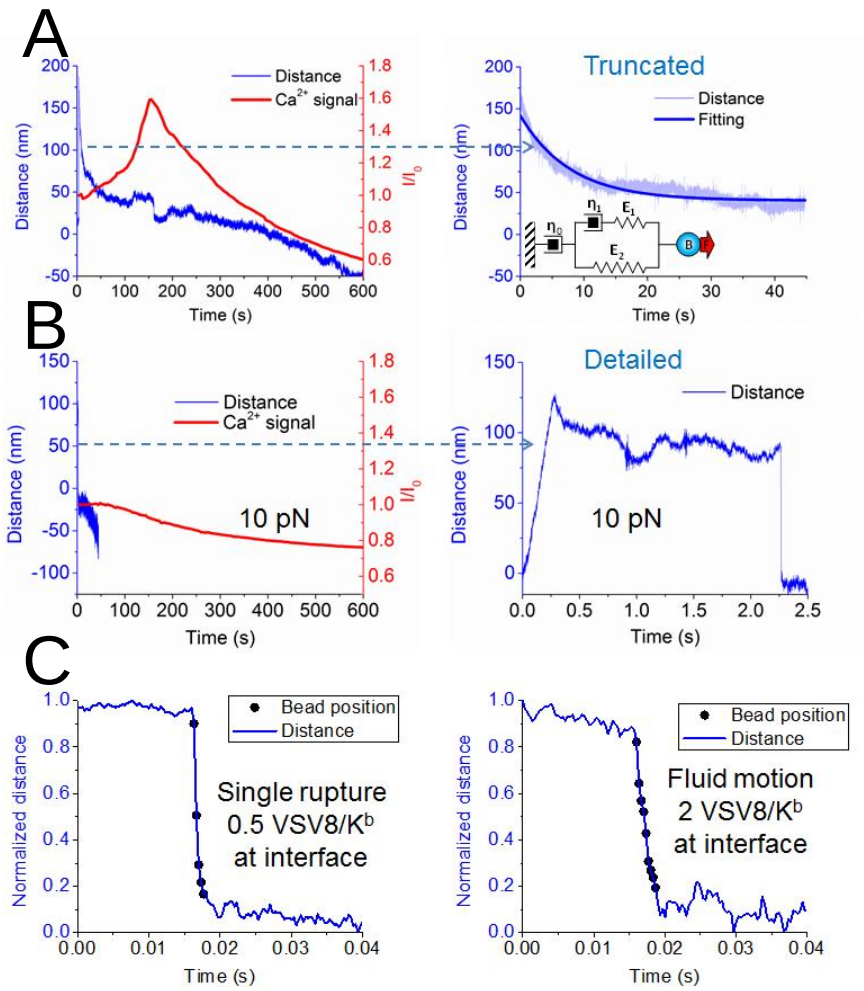

Fig. S7. Fitting procedure for force relaxation time calculation and representative traces for T cell triggering under 10 pN shear force and individual VSV8/K^b molecules at the interface.

(A) Original and truncated traces and fitting curve (navy) based on exponential decay equation associated with T cell activation for a bead type with an average of 29 VSV8/K^b at the interface. Detailed fitting steps are: 1) finding the peak position, 2) obtaining the 1st derivative from peak to end, 3) truncating the data which shows the zero derivative and 4) fitting the truncated data to the model: Distance $_{released}$=A*$e^{-t/\tau}$, τ: relaxation time(s), t: time (s), A: Initial distance between trap and bead (nm)

(B) Representative trace for 0.5 VSV8/K^b bead along shear direction showing single bond rupture and no T cell activation.

(C) Normalized representative traces for 0.5 VSV8/K^b bead (left) along shear direction showing single bond rupture with five data points and 2 VSV8/K^b bead (right) along shear direction showing fluid-like motion with eight data points and no T cell activation. Data points are separated by 1/3 ms.

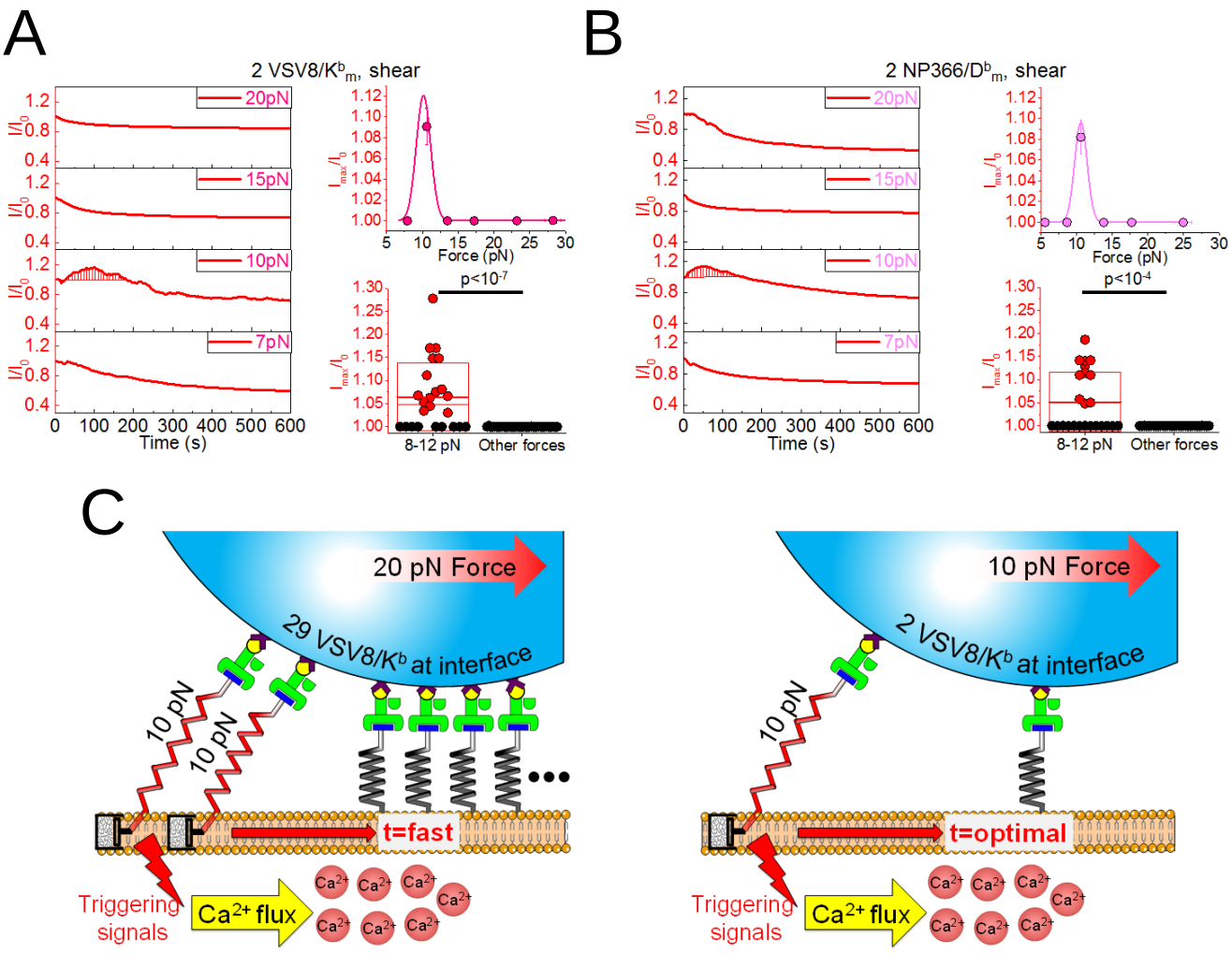

Fig. S8. External shear force-induced TCR triggering does not need engagement of the CD8 co-receptor with the same activating pMHC ligand.

(A) N15 TCR triggering in the absence of CD8 co-receptor ligation to ~2 VSV8/K^b_m at the bead-T cell interface. *p*-value referring significant analysis was evaluated using One-Way ANOVA. Triggered and non-triggered cells are represented as red and black circles, respectively. 74 cells in total were used.

(B) NP63 TCR triggering in the absence of CD8 co-receptor ligation to ~2 NP366/D^b_m at the bead-T cell interface. *p*-value referring significant analysis was evaluated using One-Way ANOVA. Triggered and non-triggered cells are represented as red and black circles, respectively. 45 cells in total were used.

(C) Cartoon of shear force facilitated αβTCR triggering. The red force arrow illustrates the force vector. Each αβTCR complex is represented as a spring. Force-loaded TCRs are in red and force-free TCRs are in

grey. To simplify, we omit the 23 no force-loaded TCR-pMHC complexes for 29 VSV8/K^b as well as non-bounded TCRs. Along the shear direction, when external force is applied on the bead, the TCRs at the back edge sense most of the pulling force, leading to $\alpha\beta$TCR triggering with 10 pN optimal force and favorable relaxation time.

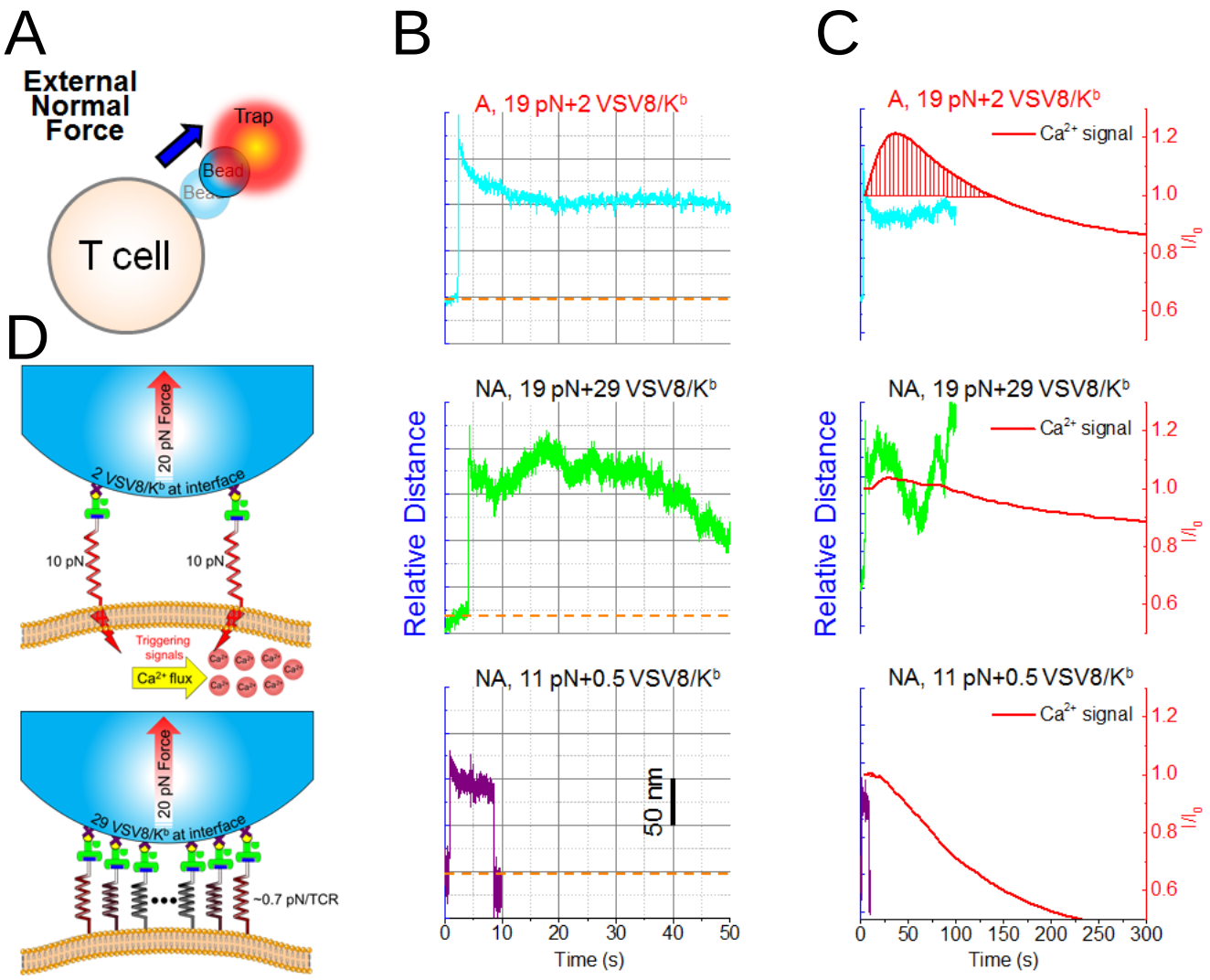

Fig. S9. Force facilitated αβTCR triggering along the normal direction.

(A) Cartoon showing partial normal force relaxation (blue arrow).

(B) Representative traces for 2 VSV8/K^b (cyan), 29 VSV8/K^b (green), and 0.5 VSV8/K^b (purple) at the bead-cell contact area. Orange dash line shows the position of the trap center.

(C) Bead displacement and Ca^{2+} signal. Optimal external trapping force along the normal direction with concurrent measurement of Ca^{2+} flux in an activated T cell (top) in comparison with absent T cell activation due to insufficient force (middle) and single bond rupture (bottom) at the contacting interface. Activation is illustrated by the area of red bars under the Ca^{2+} signal curves.

(D) Cartoon of normal force facilitated αβTCR triggering. The arrow illustrates the force vector with αβTCR shown as a spring. Force-loaded TCRs are in red and relatively force-free TCRs are in grey with omission of unbound TCRs. While complete fast relaxation is dispensable, optimal 10 pN force per TCRαβ-pMHC interaction is essential. Thus 20 pN loaded on ~2 TCRαβ-pMHC interactions using 2 VSV8/K^b beads offers each TCR a 10 pN force whereas the same force magnitude loaded on ~29 interactions distributes too little force (~0.7 pN) per complex.

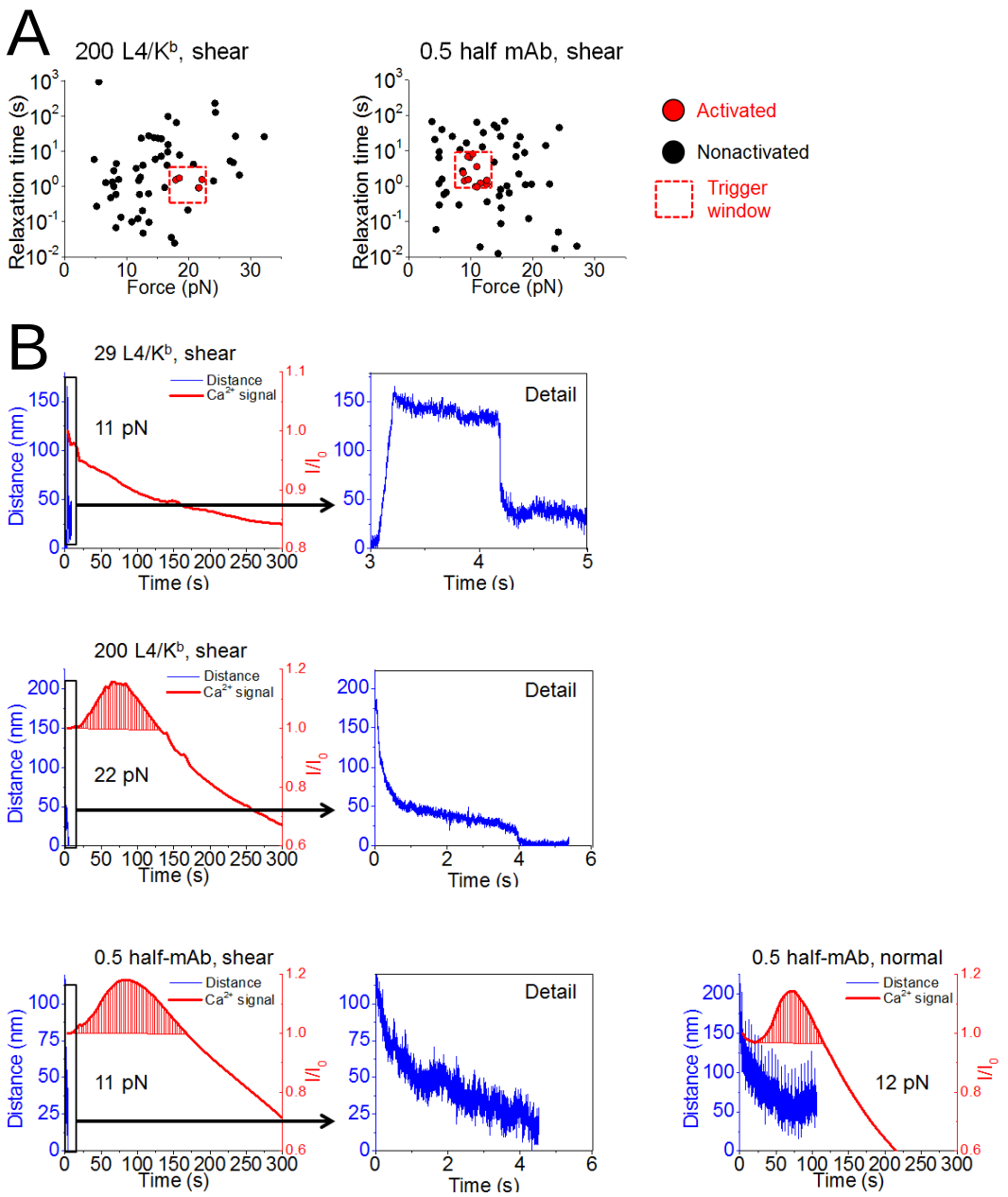

Fig. S10. Relaxation vs. force and calcium response of N15 T cells with L4/K^b and half mAb stimulation.

(A) Relationship between activation force and relaxation time for 200 L4/K^b (left) and 0.5 half anti-TCRVβ antibody (MR 9.4) (right). Note the trigger window for the half mAb is similar to **Fig. 3C** with 2 antigen pMHC coated beads.

(B) Typical traces showing bond rupture and no stimulated Ca^{2+} flux when using 29 interfacial L4/K^b (top row), whereas 200 L4/K^b along shear direction (middle row) and 0.5 half anti-TCRVβ antibody (MR 9.4) along both shear and normal directions (bottom row) induced robust Ca^{2+} flux when optimal forces were applied.

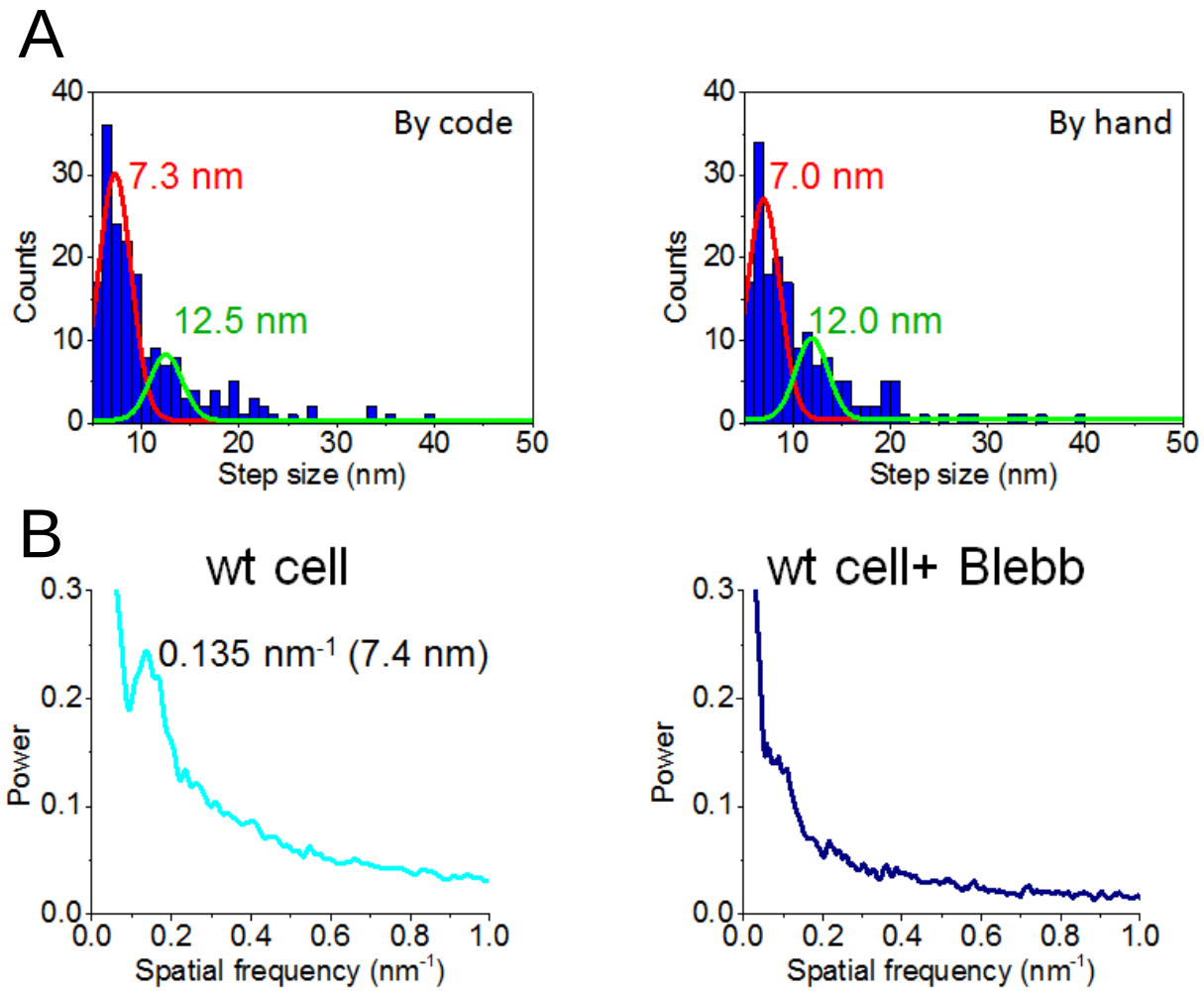

Fig. S11. Detailed step distribution characterization for N15 T cell.

(A) Step distribution comparison between step-finding code (left) and hand selection of dwell locations (right) for 18 traces.

(B) Power spectrum density analysis for wt N15 T cell and Blebbistatin (Blebb) treated cells under the conditions in **Fig. 4**. Curve of wt N15 T cell shows a visible spatial frequency peak at 0.135 nm^{-1}, which corresponds to 7.4 nm. However, Blebb treatment abolishes distinct peak exhibiting a relatively smooth curve.

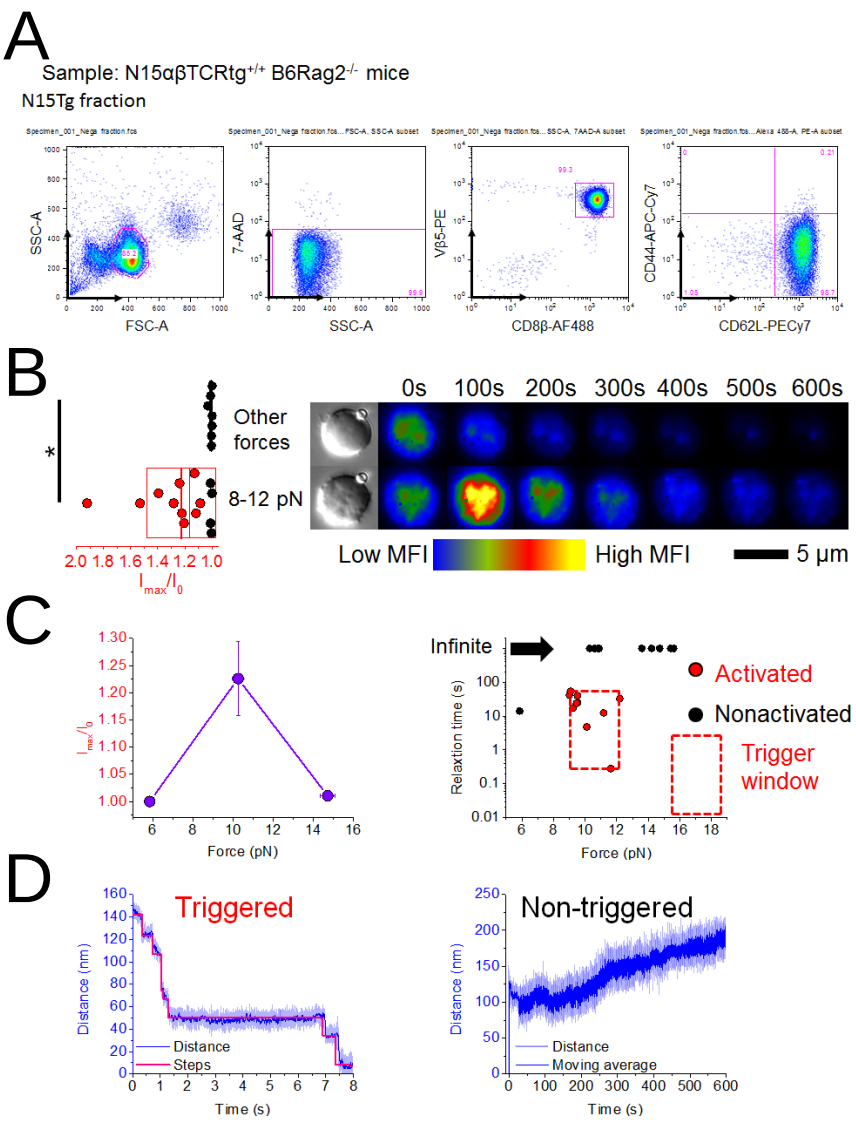

Fig. S12. Naïve N15Tg CD8$^+$ T cells from N15tg$^{+/+}$RAG2$^{-/-}$B6 mice show a similar triggering behavior as N15 T cell transfectants with respect to shear load and 2 VSV8/K^b per bead-cell interface.

(A) Naïve N15tg T cells were fluorescently stained with CD8 β–AF488 (eBioscience), Vβ 5.1/ 5.2-PE (BioLegend), CD44-APC-Cy7 (BioLegend), and CD62L-PE-Cy7 (BioLegend) and analyzed by flow cytometry using the BD LSRII. Cell debris and dead cells were excluded from the analysis based on scatter signals and 7-Aminoactinomycin D (BD Biosciences) fluorescence. The Data was analyzed by FlowJo software (Tree Star Inc.). FACS gating analysis was performed from left to right on the delineated populations. Note that essentially all CD8$^+$Vβ5$^+$ tg T cells are naïve (CD44$^-$CD62L$^+$).

(B) Ca^{2+} flux was triggered in naïve N15Tg $CD8^{+}$ T cells at 9-12 pN. *$P \leq 0.05$. *p*-value referring significant analysis was evaluated using One-Way ANOVA. Triggered and non-triggered cells are represented as red and black circles, respectively.

(C) T cell activation of Ca^{2+} flux under different load (left) and the relationship between activation force and relaxation time (right). Error bars represent SEM.

(D) Typical triggered trace showing fast relaxation via steps (left) whereas non-triggered T cells manifest no relaxation in the trace (right).

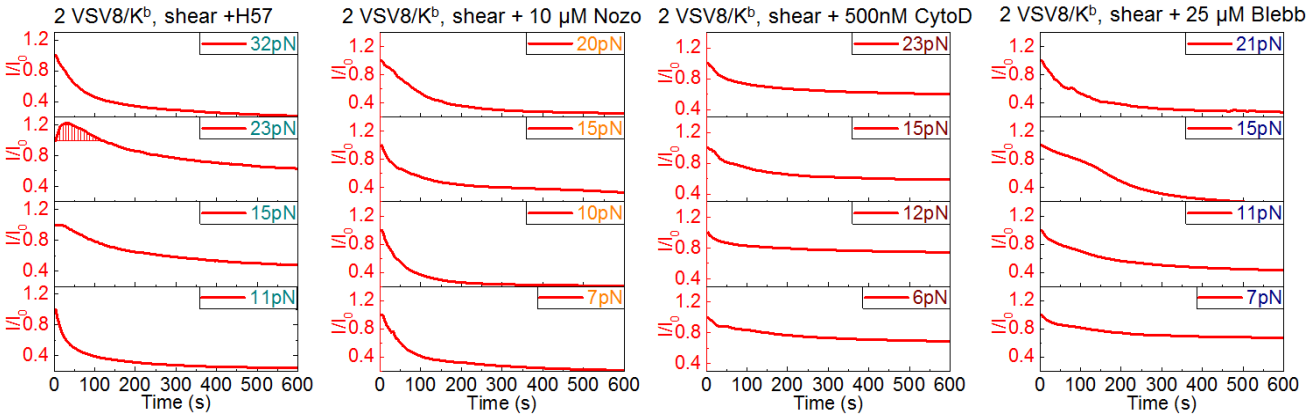

Fig. S13. External shear force-induced TCR triggering requires an intact cytoskeleton network. Representative Ca^{2+} signal for N15 T cells treated with a saturating amount of H57 Fab and or indicated drugs at the specified concentrations when using ~2 VSV8/K^b copies at interface. Activation is illustrated by the red bars under the red Ca^{2+} signal curve.

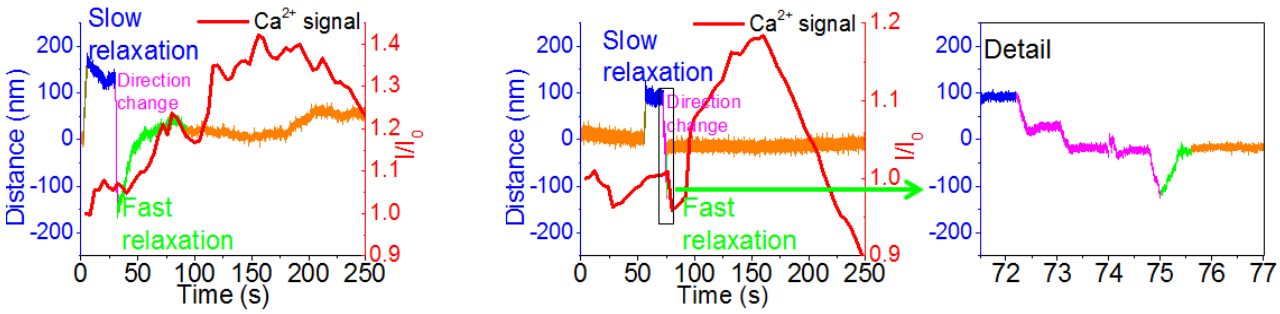

Fig. S14. Examples of triggering rescue through switching the direction of applied force from the optical trap. Pulling started at the orange portion at time zero that represents the trap center, followed by a failed TCR triggering by 29 VSV8/K^b beads after a slow relaxation (in blue) lacking Ca^{2+} flux (red curve). The event can be rescued by quickly switching the pulling force direction (in magenta). This directional change induces fast relaxation (in green) and attendant Ca^{2+} flux (red curve). A detail blowup of the second example is shown in the far right panel.

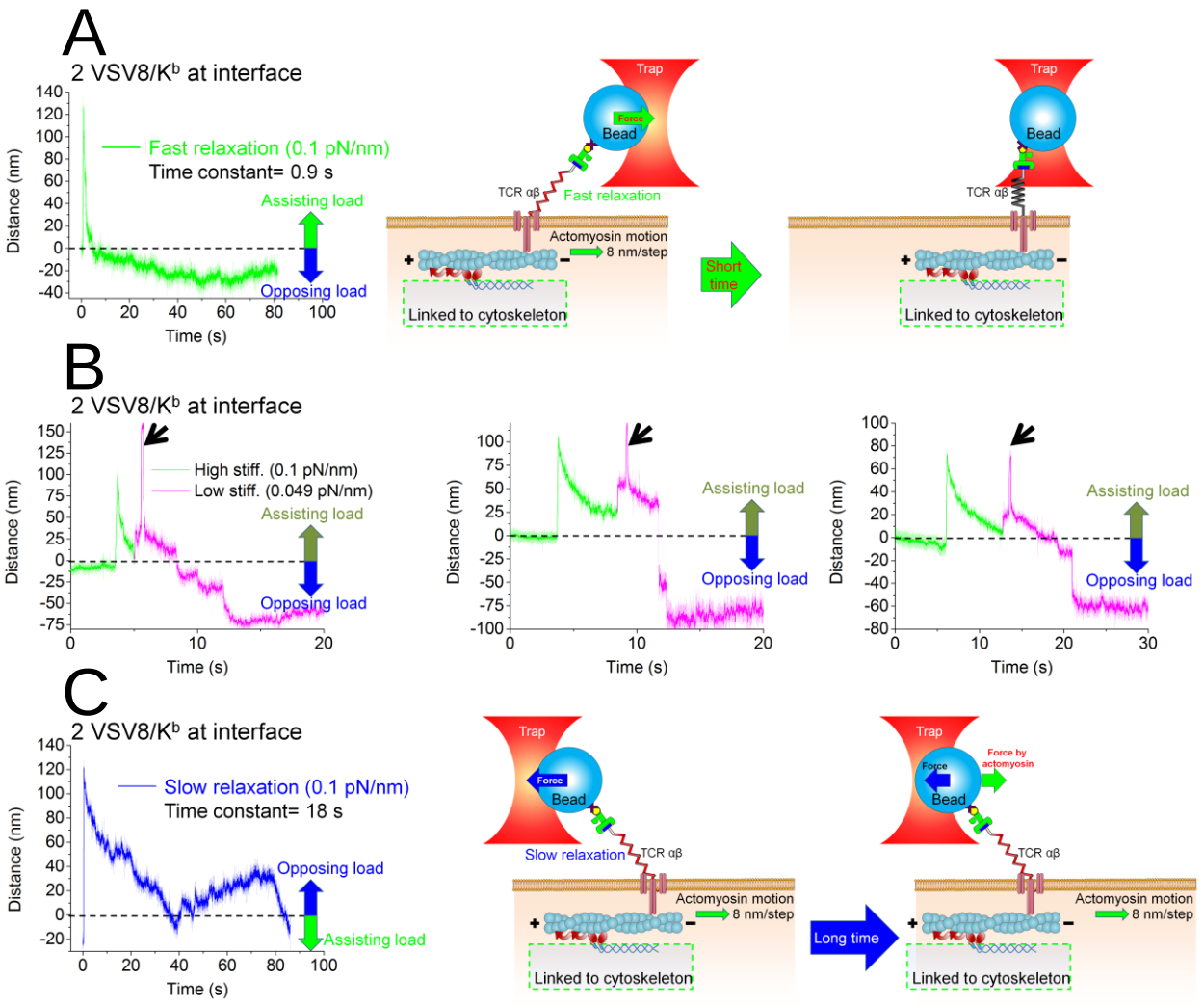

Fig. S15. Representative traces for force relaxation and a possible mechanism linked to T cell functional activation when using ~2 pMHC copies are at interface. Black dash in each trace represents trap center.

(A) Fast relaxation at 0.1 pN/nm stiffness. When force direction (in green) is consistent with the actomyosin motion (in green), the TCR may be extended initially but is then restored to its original geometry as the bead rapidly returns to trap center due to actomyosin motion. Note the bead continues moving against the opposing load and stalls at ~3.7 pN.

(B) Representative traces showing possible active transport of the bead with longer displacement against the opposing load when lowering down the trap stiffness (black arrow) after the cell activation. The stall force is still ~3.7 pN. In these experiments cells were triggered at higher trap stiffness (0.1 pN/nm, green) and then the trap force was reduced to a lower stiffness (0.049 pN/nm, pink). Note that

there is a spike soon after the trap stiffness change due to a brief period where the acoustic-optic deflector amplitude is adjusting to the new setting. In the presence of the weaker trap, the system transitions to an opposing load geometry and pulls the bead out of the trap. In these cases the magnitude of displacement is larger showing directed motion still continues against the trap force. The maximum displacements are consistent with measured stall force.

(C) Slow relaxation at 0.1 pN/nm stiffness. In this case force direction (in blue) is against the actomyosin motion (in green) so that the initially extended TCR remains extended with the bead returning slowly to the trap center. Note at the trap center (~0 nm distance) the bead moves in the other direction, stalling at 3.77±0.50 pN (n=30) due to the “tug of war” between actomyosin motion and trapping forces.

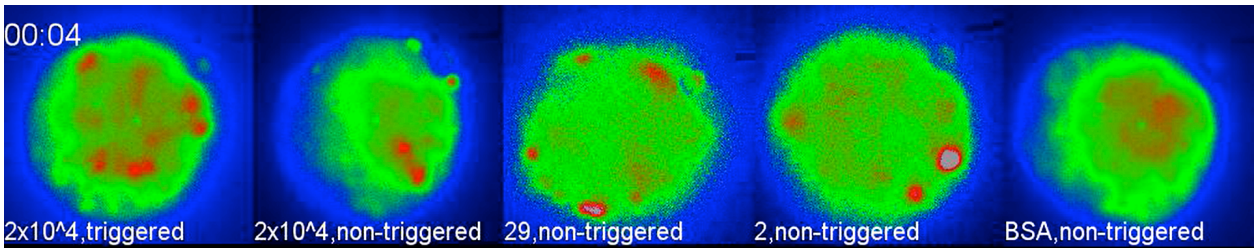

Movie S1. Ca^{2+} flux was triggered by high number (~2×10^4) but not physiological number (29 and 2) of VSV8/K^b at interface without external force. Left to right are 2×10^4 VSV8/K^b/triggered, 2×10^4 VSV8/K^b/nontriggered, 29 VSV8/K^b/nontriggered, 2 VSV8/K^b/nontriggered and BSA/nontriggered.

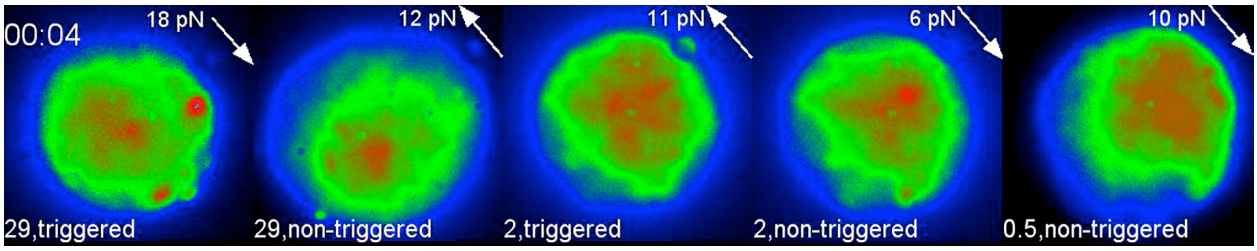

Movie S2. Optimal external shear force can trigger Ca^{2+} flux by physiological number (29 and 2) of VSV8/K^b at interface. Left to right are 29 VSV8/K^b + 18 pN/triggered, 29 VSV8/K^b + 12 pN/nontriggered, 2 VSV8/K^b + 11 pN/triggered, 2 VSV8/K^b + 6 pN/nontriggered, 0.5 VSV8/K^b + 10 pN/nontriggered. Arrow shows the direction of the force.

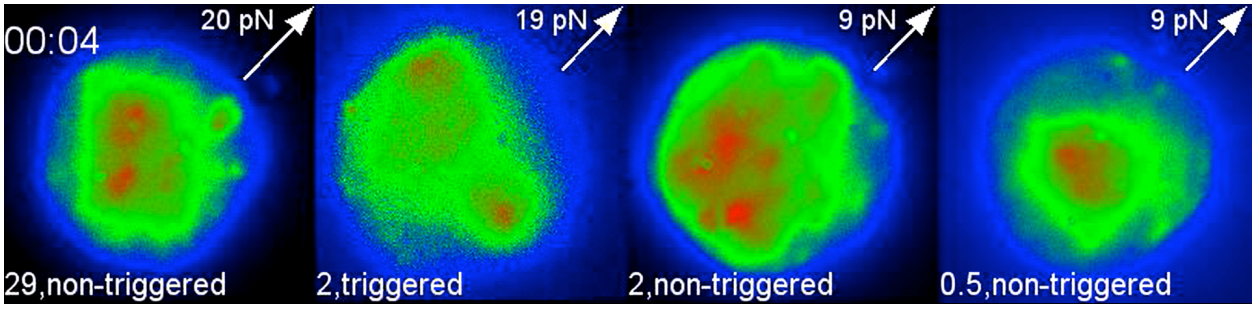

Movie S3. Optimal external normal force can trigger T cell Ca^{2+} flux with as few as 2 VSV8/K^b molecules at the interface. Left to right are 29 VSV8/K^b + 20 pN/nontriggered, 2 VSV8/K^b + 19 pN/triggered, 2 VSV8/K^b + 9 pN/nontriggered and 0.5 VSV8/K^b + 9 pN/nontriggered. Arrow shows the direction of the force.

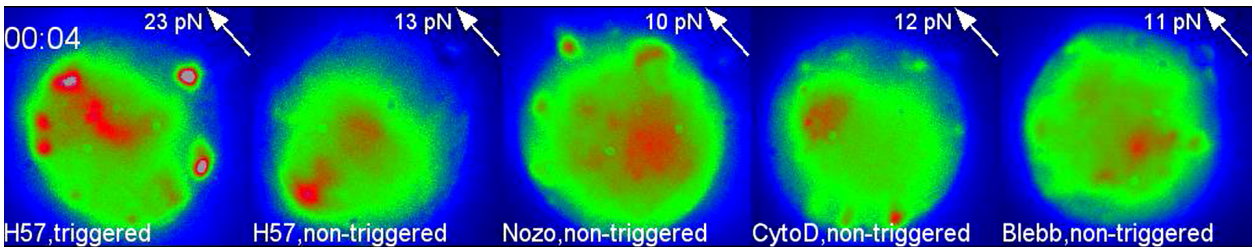

Movie S4. Ca^{2+} flux of H57 Fab or drug loaded T cells pulled by 2 of VSV8/K^b at interface. With H57 Fab, higher external shear force is needed to trigger Ca^{2+} flux, which has short duration. Left to right are H57 Fab + 23 pN/triggered, H57 Fab + 13 pN/nontriggered, 10 μM Nocodazole + 10 pN/nontriggered, 500 nM Cytochalasin D + 12 pN/nontriggered and 25 μM Blebbistatin + 11 pN/nontriggered. Arrow shows the direction of the force.

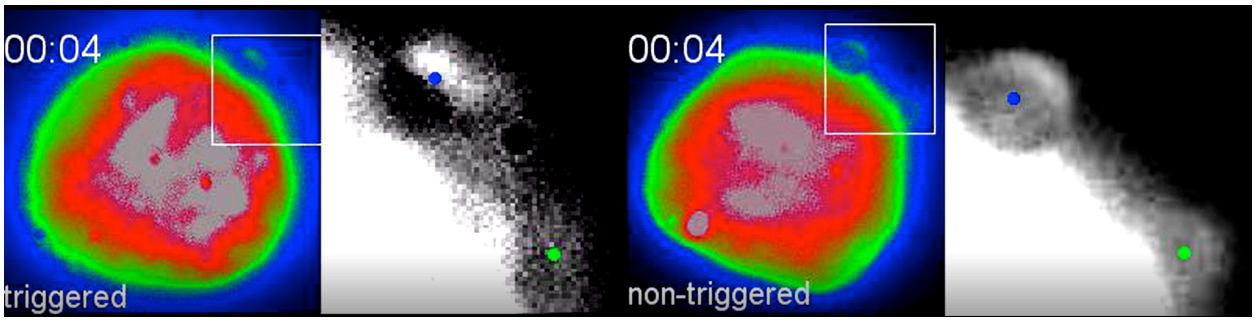

Movie S5. During TCR triggering, more N15 αβTCRs (marked by lower bead with green dot, 1.03 μm) will be gathered to the interface where the triggering initiates (Upper bead with blue dots, 1.25 μm) to magnify the triggering signal (1st and 2nd columns) whereas nontriggered cells showing limited αβTCR motion (3rd and 4th columns). 2nd and 4th columns are zoomed in from two beads region in 1st and 3rd column, respectively.